Fourier transform spectroscopy of d-wave quasiparticles in the presence of atomic scale pairing disorder

Tamara S. Nunner, Wei Chen, Brian M. Andersen, Ashot Melikyan, and P. J. Hirschfeld
Department of Physics, University of Florida, Gainesville, FL 32611, USA
(Dated: December 21, 2005)

The local density of states power spectrum of optimally doped $Bi_2Sr_2CaCu_2O_{8+x}$ (BSCCO) has been interpreted in terms of quasiparticle interference peaks corresponding to an "octet" of scattering wave vectors connecting **k**-points where the density of states is maximal. Until now, theoretical treatments have not been able to reproduce the experimentally observed weights and widths of these "octet" peaks; in particular, the predominance of the dispersing "$\mathbf{q_1}$" peak parallel to the Cu-O bond directions has remained a mystery. In addition, such theories predict "background" features which are not observed experimentally. Here, we show that most of the discrepancies can be resolved when a realistic model for the out-of-plane disorder in BSCCO is used. Weak extended potential scatterers, which are assumed to represent cation disorder, suppress large-momentum features and broaden the low-energy "$\mathbf{q_7}$"-peaks, whereas scattering at order parameter variations, possibly caused by a dopant-modulated pair interaction around interstitial oxygens, strongly enhances the dispersing "$\mathbf{q_1}$"-peaks.

PACS numbers: 74.25.Bt,74.25.Jb,74.40.+k

I. INTRODUCTION

For several years, high-resolution scanning tunnelling microscopy (STM) experiments [1, 2, 3, 4, 5, 6, 7, 8, 9, 10, 11, 12, 13, 14] have been imaging the local electronic structure of cuprate superconductors. These experiments have discovered resonant defect states [1, 2, 3] and revealed the existence of nano-scale inhomogeneities [4, 5, 6, 7]. From a highly disordered spatial tunneling signal, it has become standard to use Fourier transform scanning tunnelling spectroscopy (FT-STS) [15] techniques to extract, e.g., the characteristic wavelengths of Friedel-type oscillations [16] and, if present, the background charge order. In a simple metal, the local density of states around an impurity varies as $\sim \cos 2k_F r/r^3$, so the wavelength of the local density of states (LDOS) "ripples" caused by a single impurity is a measure of the Fermi wave vector of the pure system [15]. In the quasi-2D d-wave superconductor, the spherical shell of maximum FT-STS intensity with radius $2k_F$ is replaced by a discrete set of peaks at positions $\mathbf{q}_\alpha$, $\alpha = 0...7$ (see Fig. 1) which connect an octet of points of high density of states in momentum space [8, 17, 18, 19, 20, 21]. The fact that in optimally doped BSCCO the measured dispersion of these peaks with STM bias [8, 12, 13] agrees semi-quantitatively with the predictions based on d-wave BCS-theory is considered as strong evidence for the existence of well-defined quasiparticles in the superconducting state of optimally doped cuprate superconductors, and for the applicability of d-wave BCS-theory in this regime. Recent attempts to relate ARPES spectral functions to STM Fourier transform patterns have met with reasonable success, supporting this conclusion [22, 23, 24].

At lower doping, the dispersing peaks are still present, but additional nondispersing peaks are observed corresponding to wave vectors along the Cu-O bonds with wavelength close to four lattice spacings [13, 14]. Nondispersing peaks have been reported in overdoped samples as well, and have been discussed in terms of stripelike charge ordering [9, 10]. The nature and degree of charge ordering and the existence of the nondispersive peaks in these materials is still controversial, however. In this work we neglect charge ordering and discuss exclusively the Fourier transform LDOS response of the d-wave superconducting state to disorder.

Despite the overall success of interpreting the Fourier STM patterns in terms of quasiparticle interference, none of the existing models has been able to correctly account for the observed weights and widths of the dispersive q-space peaks. The pointlike single-impurity theories [8, 17, 18, 19, 20, 21] yield peak structures which are sharp, and linear or arclike in structure, in contrast to the experimental features, which appear as a series of broad, roughly round spots. Depending on the assumed form of the impurity potential and its strength, the relative intensity weights of the different octet peaks change, but there has been no choice of potential found which adequately accounts for the experimentally observed weights. In particular, all such calculations appear to drastically underestimate the weight of the dispersing $\mathbf{q}_1$-peaks and in contrast to experiment predict many "background" features, i.e., strong intensity in regions of q-space other than the octet peaks.

Many-impurity calculations with weak scatterers displayed some of the same features as the single-impurity calculations, and showed how increasing disorder eventually swamps the octet peaks by raising the noise floor, but were not notably more successful in reproducing the experimental FT-STS patterns [25]. It was therefore suggested by Zhu *et al.* [26] that it is essential to consider a more realistic disorder model for BSCCO, including the effect of roughly 0.2% in-plane native defects, which are generally considered as strong pointlike scatterers due to the resonances they generate near zero bias [11], as well

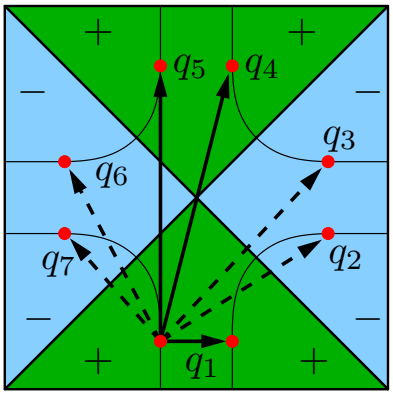

FIG. 1: Schematic depiction of the first Brillouin zone in cuprate superconductors. Green (blue) regions represent $\Delta_{\mathbf{k}} > 0$ ($\Delta_{\mathbf{k}} < 0$). Red dots are intersections of constant quasiparticle energy contours with the Fermi surface. The fraction of octet vectors, $\mathbf{q}_1$, $\mathbf{q}_4$, $\mathbf{q}_5$ which should in principle be visible in the case of a "pointlike" (4-bond) τ_1-scatterer are denoted with solid lines, the remaining octet vectors are indicated with dashed lines.

as the effect of out-of-plane defects, which most likely act as weak extended scatterers due to poor screening within the CuO_2-planes. Using this disorder model Zhu *et al.* were able to reproduce the experimental FT-STS patterns at low biases of order 10-15meV reasonably well, but at higher energies agreement was rather poor. They attributed the low-energy behavior to the in-plane native defects and interpreted the role of the extended weak out-of-plane scatterers as broadening the octet peaks. A broadening of small-momentum features has also been reported by Dell'Anna *et al.* [27] due to mesoscopic inhomogeneities.

In this paper we show that a realistic treatment of the out-of-plane disorder plus the consideration of in-plane native defects is necessary to understand the key features of the experimental Fourier transform patterns. There are at least two major sources of out-of-plane disorder in this material: (i) non-stoichiometric oxygen dopant atoms and (ii) random substitution of Bi at the Sr-sites [28]. Very recently, direct information on both types of impurities has been obtained by STM. Kinoda *et al.* [29] succeeded in imaging the excess Bi^{3+} at a bias of 1.7 eV, finding an areal concentration of about 3%, consistent with earlier estimates from bulk measurements [28]. In addition, McElroy *et al.* [30] imaged a set of atomic scale defects at -0.96 eV, whose concentration scales with doping. These defects, which were ultimately identified as the interstitial oxygen dopant atoms, were shown to correlate strongly and positively with the local gap size in the superconducting state.

We have recently suggested that the above mentioned experimental observations can be understood based on the simple assumption that the main effect of the interstitial dopants (i.e. disorder (i)) is to increase the pair interaction locally [31]. This assumption yields gap modulations which correlate positively with the dopant positions, gives rise to particle-hole symmetric spectra and suppresses high-energy coherence peaks as observed in experiment. The underlying assumption is that each interstitial oxygen distorts the "cage" of atoms around it, thereby modulating the pair interaction locally. Alternatively, these order parameter modulations could also arise from sources other than microscopic pairing disorder, e.g. via coupling of ordinary electrostatic impurity potentials to phases which compete with d-wave superconductivity, see e.g. Ref. [32]. Nevertheless, the phenomenological assumption of microscopic pairing disorder has already proven successful with respect to many experimental observations in BSCCO. Scattering by order parameter variations has been reported to improve dramatically the fit to the inelastic tunneling spectroscopy experiments [33]. Fang *et al.* [34] reported very sharp coherence peaks in small gap regions consistent with an Andreev bound state in a region of suppressed order parameter, as discussed in Ref. [31]. Very recently, J.-X. Zhu explored the effect of dopant modulated Cu-Cu hopping within a Bogoliubiov-de Gennes framework [35]. Finally, order parameter modulations with a phase twist have been found to yield low-energy impurity bound state energies and a spatial distribution of the LDOS similar to those observed near Zn-impurities in BSCCO-2212 [36]. Thus it is intriguing to explore the consequences of this unusual quasiparticle scattering from the order parameter modulations further, in particular its effect on the FT-STS patterns.

Unlike the oxygen dopants, the Bi^{3+} defects, i.e. disorder component (ii), most likely act as conventional weak and extended potential scatterers due to the different charge of the Sr- and Bi-ions and the smaller deformation of the lattice itself. The existence of a large concentration of extended weak potential scatterers is also supported by an analysis of transport properties in BSCCO [37].

The final aspect of the disorder we discuss is the small concentration of in-plane native defects, about 0.2% per Cu, imaged by STM [11]. It is believed that these are Cu vacancies in the CuO_2 plane, although no direct proof exists. Individually, these defects provide a resonant signal centered within 1 meV of the Fermi level similar but not identical to Zn. The resonance modulates the LDOS primarily below 15 meV or less, and then furthermore at energies not far from the gap edge where the resonant spectral weight originates. We model these defects as strong pointlike unitary potential scatterers, as in Zhu *et al.* [26], noting that because the concentration and resonance energies of these defects are known from experiment, they do not introduce new model parameters.

Thus, we believe that a realistic model of the disorder in BSCCO should contain a net out-of-plane disorder consisting of extended weak potential scatterers (approx. 3%, i.e., the concentration of Bi-defects) and extended off-diagonal scatterers (approx. 7.5%, i.e., half the doping, because each oxygen dopant most likely contributes

two holes) plus a concentration of 0.2% pointlike and strong in-plane defects. It is the purpose of this paper to investigate the effect of these three disorder components on the FT-STS patterns.

II. MODEL

As a model for the homogeneous system we use the usual BCS Hamiltonian given by

$$\mathcal{H}_0 = \sum_{\mathbf{k},\sigma} \varepsilon_{\mathbf{k}} \hat{c}^\dagger_{\mathbf{k}\sigma} \hat{c}_{\mathbf{k}\sigma} + \sum_{\mathbf{k}} \left(\Delta_{\mathbf{k}} \hat{c}^\dagger_{\mathbf{k}\uparrow} \hat{c}^\dagger_{-\mathbf{k}\downarrow} + \text{H.c.} \right), \quad (1)$$

where $\varepsilon_{\mathbf{k}}$ is the quasiparticle dispersion proposed to fit the ARPES data [38]: $\varepsilon_{\mathbf{k}} = \sum_{n=0}^{5} t_n \chi_n(k)$, where $t_{0-5} = 0.1305, -0.5951, 0.1636, -0.0519, -0.1117, 0.0510$ (eV), and $\chi_{0-5}(k) = 1$, $(\cos k_x + \cos k_y)/2$, $\cos k_x \cos k_y$, $(\cos 2k_x + \cos 2k_y)/2$, $(\cos 2k_x \cos k_y + \cos 2k_y \cos k_x)/2$, and $\cos 2k_x \cos 2k_y$. For d-wave pairing we have, $\Delta_{\mathbf{k}} = 2\Delta_0(\cos k_x - \cos k_y)$ with $\Delta_0 = 12$meV.

In terms of the Nambu spinor $\hat{\psi}^\dagger_{\mathbf{k}} = (\hat{c}^\dagger_{\mathbf{k}\uparrow}, \hat{c}_{-\mathbf{k}\downarrow})$, the corresponding bulk Green's function in Matsubara representation is given by

$$\mathcal{G}^0(\mathbf{k}, i\omega_n) = \frac{i\omega_n \tau_0 + \xi_{\mathbf{k}} \tau_3 + \Delta_{\mathbf{k}} \tau_1}{(i\omega_n)^2 - E^2_{\mathbf{k}}}, \quad (2)$$

where $E^2_{\mathbf{k}} = \xi^2_{\mathbf{k}} + \Delta^2_{\mathbf{k}}$, and τ_0 is the 2×2 identity matrix, whereas (τ_1, τ_2, τ_3) denote the three Pauli matrices. In real-space, the perturbation due to the conventional point-like potential scatterers in the diagonal τ_3 channel and modulated pairing amplitude in the off-diagonal τ_1 channel can be written as

$$\mathcal{H}'(\mathbf{r}, \mathbf{r}') = \hat{\psi}^\dagger_{\mathbf{r}} \left[V(\mathbf{r} - \mathbf{r}') \delta(\mathbf{r} - \mathbf{r}') \tau_3 + \delta\Delta(\mathbf{r}, \mathbf{r}') \tau_1 \right] \hat{\psi}_{\mathbf{r}'}. \quad (3)$$

Note that the conventional impurity scattering occurs with Pauli matrix τ_3 in (3), whereas the order parameter modulation, or Andreev scattering term, occurs with τ_1. We will henceforth adopt the convenient shorthand of referring to the two types of processes as τ_3 or τ_1 disorder, respectively.

We use a Yukawa form to model the extended conventional potential of an out-of-plane defect:

$$V(\mathbf{r}) = \frac{V_0 r_z}{e^{-r_z/\lambda}} \frac{e^{-d/\lambda}}{d} \quad \text{with} \quad d = \sqrt{r^2 + r_z^2}, \quad (4)$$

where $\mathbf{r}$ is an in-plane vector, r_z is the distance of the defect from the CuO_2-plane and the potential is normalized to V_0 in the CuO_2-plane directly below the defect. An extended τ_1-scatterer is modeled by using the same functional form in the τ_1 channel as

$$\delta\Delta(\mathbf{r}, \mathbf{r}') = \frac{\delta\Delta\, r_z}{e^{-r_z/\lambda}} \frac{e^{-d/\lambda}}{d} \text{ with } d = \sqrt{(\frac{1}{2}(\mathbf{r} + \mathbf{r}'))^2 + r_z^2}\,. \quad (5)$$

We note that there is no microscopic justification for this form, nor any direct connection with a physical screened Coulomb potential; this is merely a convenient way to introduce a length scale to the order parameter modulations induced by the dopant atoms.

In order to determine the resulting LDOS as a function of energy and lattice sites, one needs to obtain the full Green's function $\mathcal{G}(\mathbf{r}, \mathbf{r}', i\omega_n)$ given by the Dyson equation

$$\mathcal{G}(\mathbf{r}, \mathbf{r}') = \mathcal{G}^0(\mathbf{r} - \mathbf{r}') + \sum_{\mathbf{r}'', \mathbf{r}'''} \mathcal{G}^0(\mathbf{r} - \mathbf{r}'') H'(\mathbf{r}'', \mathbf{r}''') \mathcal{G}(\mathbf{r}''', \mathbf{r}'). \quad (6)$$

Thus, by calculating

$$\mathcal{G}^0(\mathbf{r}, i\omega_n) = \sum_{\mathbf{k}} \frac{(i\omega_n \tau_0 + \xi_{\mathbf{k}} \tau_3 + \Delta_{\mathbf{k}} \tau_1)}{(i\omega_n)^2 - E^2_{\mathbf{k}}} \exp(i\mathbf{k} \cdot \mathbf{r}), \quad (7)$$

the remaining problem is that of a simple matrix inversion, and the LDOS $\rho(\mathbf{r}, \omega)$ can be extracted from the imaginary part of the full Green's function, $\rho(\mathbf{r}, \omega) = -\frac{1}{\pi} \text{Im} \mathcal{G}_{11}(\mathbf{r}, \mathbf{r}, \omega)$.

III. RESULTS

We now examine the effect of a single scatterer on the FT-STS patterns. The philosophy of calculations of this type [17, 18] is simply that the "Friedel oscillations" in the d-wave quasiparticle sea around a single impurity will contain many of the wavelengths present in the fully disordered system. The FTDOS due to the impurity is then given by

$$\rho(\mathbf{q}, \omega) = \sum_{\mathbf{r} \in L \times L} e^{-i\mathbf{q} \cdot \mathbf{r}} \rho(\mathbf{r}, \omega) \quad (8)$$

where $L \times L$ is a square set of L^2 positions at which measurements are made, and $\mathbf{q} = 2\pi(m, n)/L$ are vectors in the associated reciprocal lattice. The power spectrum [39] is simply the 2D image obtained from the amplitude $|\rho(\mathbf{q}, \omega)|$. In the case that several disorder components are present we calculate the power spectrum as $|\rho(\mathbf{q}, \omega)| = |\sum_i n_i \rho_i(\mathbf{q}, \omega)|$, where ρ_i and n_i denote the FTDOS and concentration of each disorder component.

Fig. 2 compares the resulting power spectra for different impurity models computed for $L = 53$. In the 1st column, the power spectrum for a weak pointlike τ_3-impurity, discussed previously in Refs. [18, 26], is reproduced. In contrast to the experimental power spectrum, the calculation for a pointlike τ_3-impurity predicts strong weight at large wavevectors especially near (π, π), which is observed experimentally only at very low frequencies. In the case of an extended τ_3-scatterer (2nd column in Fig. 2), on the other hand, the high-momentum features are suppressed due to the rapid fall-off of the impurity potential $V(\mathbf{q})$ in momentum space. This is, however, not the only difference between pointlike and extended τ_3-scatterers. The FT-patterns also change for small momenta; most noticeably, the $\mathbf{q}_7$-peaks are enhanced due to small-angle scattering of quasiparticles by the smooth

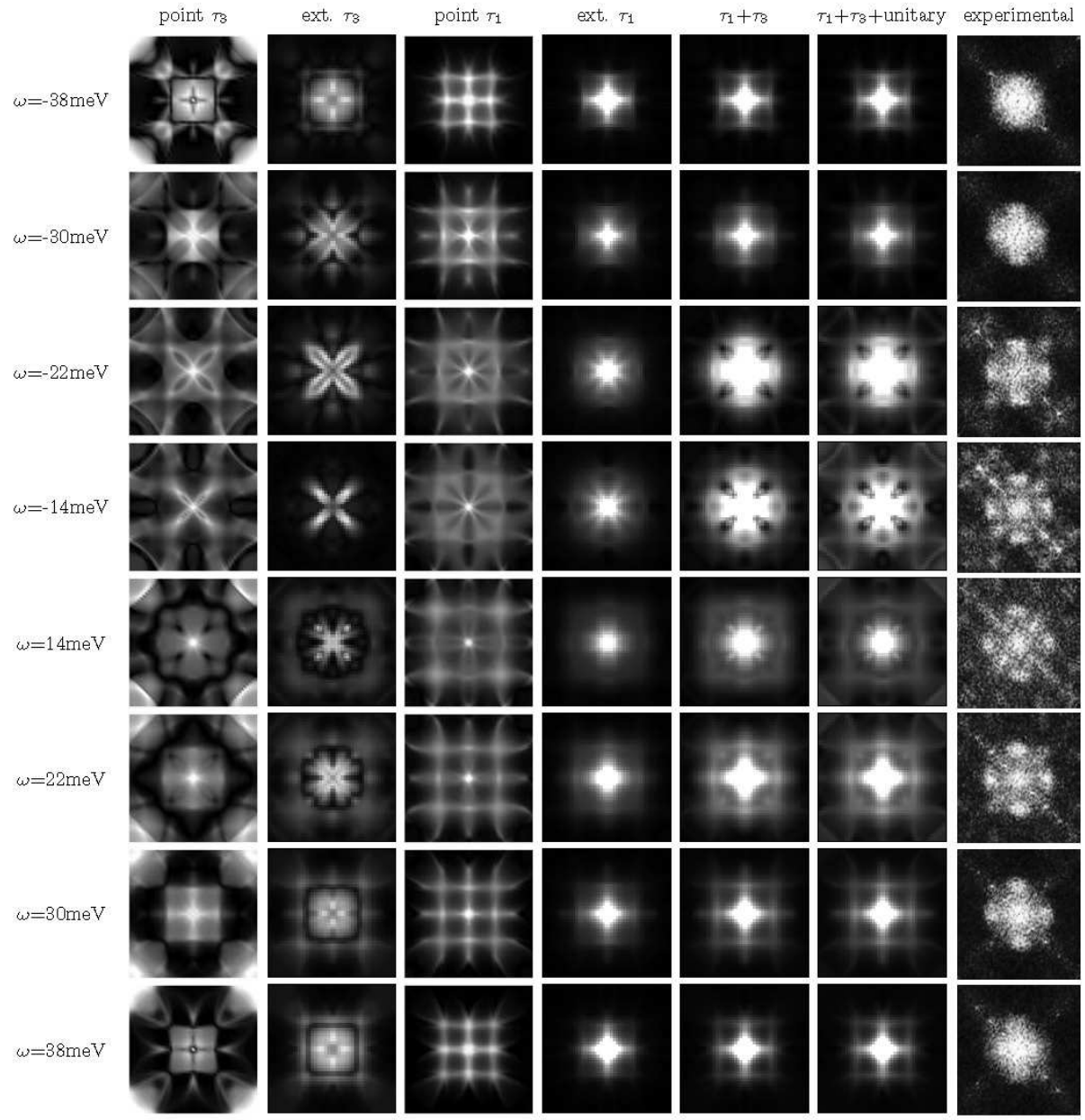

FIG. 2: Effect of out-of-plane scattering potentials of different type on the power spectrum. Shown is the power spectrum for: 1st column: pointlike τ_3-scatterer with strength V=120meV, 2nd column: extended τ_3-scatterer with V_0=40meV, $\lambda = r_z = 1.5a$, 3rd column: pointlike τ_1-scatterer with $\delta\Delta = \Delta_0$ on the four central bonds, 4th column: slightly extended τ_1-scatterer with $\delta\Delta = \Delta_0$, $\lambda = r_z = 1.2a$, 5th column: combination of 7.5% extended τ_1-scatterers ($\delta\Delta = \Delta_0$, $\lambda = r_z = 1.2a$) and 3% extended τ_3-scatterers (V_0=40meV, $\lambda = r_z = 1.5a$), 6th column: same as 5th column plus 0.2% unitary (V=3.9meV) pointlike scatterers, 7th column: experimental power spectrum [12, 13].

potential. Whereas the $\mathbf{q}_7$-peaks appear only as tiny spots in the case of a pointlike impurity [26], too small to be resolved in Fig. 2, they become broad spots in the case of an extended impurity and are clearly visible at the energies $|\omega| = 14$meV, 22meV in Fig. 2. This supports the proposal by Zhu *et al.* [26] that the enhancement of forward scattering due to spatially extended impurities broadens the octet peaks.

In addition to the existence of weak extended τ_3-scatterers, which could arise e.g. due to random substitutions of Sr by Bi, the pair interaction is most likely modulated due to the presence of non-stoichiometric oxygen dopant atoms [31]. This results in inhomogeneities in the magnitude of the superconducting order parameter and enhanced Andreev scattering which can be modeled as τ_1-scattering within a single-impurity approach. The 3rd column in Fig. 2 shows the power spectrum for a "pointlike" τ_1-scatterer, i.e., a modulation of the order parameter on the four bonds surrounding the impurity site as $\delta\Delta(0,\pm\hat{x}) = \delta\Delta(\pm\hat{x},0) = -\delta\Delta(0,\pm\hat{y}) = -\delta\Delta(\pm\hat{y},0) = \delta\Delta$. Obviously, the resulting FT-pattern looks very different from a pointlike τ_3-scatterer. The background features, i.e., the finite FTDOS at wavevectors that do not correspond to one of the octet peaks, are much less pronounced. At high energies ($|\omega| = 30$meV, 38meV), the power spectrum is clearly dominated by $\mathbf{q}_1$-peaks, whereas the $\mathbf{q}_7$-peaks are completely absent even at the lowest energies. This behavior can be understood in terms of the momentum dependence of the scattering matrix element for a "pointlike" τ_1-scatterer. Fourier transformation of the "pointlike" order parameter modulation yields

$$\delta\Delta_{\mathbf{k}\mathbf{k}'} = \delta\Delta(\Delta_{\mathbf{k}} + \Delta_{\mathbf{k}'})/\Delta_0\,, \tag{9}$$

i.e., $\delta\Delta_{\mathbf{k}\mathbf{k}'}$ vanishes for wavevectors $\mathbf{k}$ and $\mathbf{k}'$ which connect points of the Brillouin zone where $\Delta_{\mathbf{k}}$ and $\Delta_{\mathbf{k}'}$ have opposite signs but equal magnitudes. Among the octet vectors, only $\mathbf{q}_1$, $\mathbf{q}_4$ and $\mathbf{q}_5$ are allowed scattering processes contributing to the FTDOS for a "pointlike" τ_1-scatterer, whereas $\mathbf{q}_2$, $\mathbf{q}_3$, $\mathbf{q}_6$ and $\mathbf{q}_7$ are suppressed because the matrix element $\delta\Delta_{\mathbf{k},\mathbf{k}'}$ vanishes for these $\mathbf{q}$, see Fig. 1. The 4th column of Fig. 2 shows the power spectrum for the case of a slightly more extended τ_1-scatterer. The primary effect of extending the spatial range of the order parameter modulation is analogous to the τ_3-case, i.e., the intensity at large momenta and background features are suppressed resulting in even more pronounced $\mathbf{q}_1$-peaks.

The 5th column of Fig. 2 presents the power spectrum of an extended impurity with a combined τ_1- plus τ_3-potential, where each single component corresponds to the potential used for the extended τ_3/τ_1-case in the 2nd /4th column. Since we assume that the extended τ_3-scatterers result from the 3% Sr/Bi-disorder and the extended τ_1-scatterers from the 7.5% dopant oxygens the FTDOS of each component has been weighted with a prefactor corresponding to the ratio of these two concentrations. Alternatively, a scatterer with combined τ_1- and

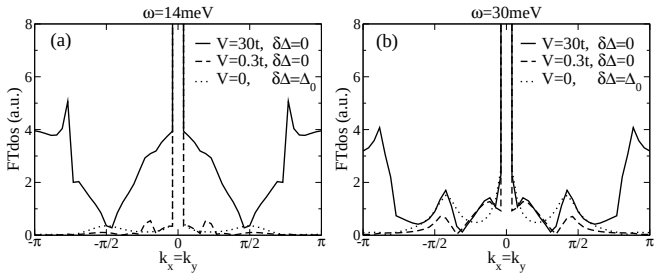

FIG. 3: Cut along the diagonal of the Brillouin zone (k_x=k_y) through the power spectrum of a strong pointlike τ_3-scatterer with V=3.9eV (solid line), a weak extended τ_3-scatterer with V_0=40meV, $\lambda = r_z$=1.5a (dashed line) and a "pointlike" τ_1-scatterer with $\delta\Delta = \Delta_0$ (dotted line) for an energy of (a) ω=14meV and (b) ω=30meV.

τ_3-character could also arise due to the fact that each oxygen dopant, besides modulating the pair potential, most likely also possesses a small but finite conventional potential component. The extended $\tau_1 + \tau_3$-case obviously combines the main characteristics of the extended τ_1 and the extended τ_3-case. At $|\omega| = 14$meV the power spectrum is dominated by $\mathbf{q}_7$-peaks, at $|\omega| = 22$meV both the $\mathbf{q}_7$- and the $\mathbf{q}_1$-peaks are present, whereas the highest frequencies $|\omega| = 30$meV and $|\omega| = 38$meV are clearly dominated by $\mathbf{q}_1$-peaks.

In addition to out-of-plane impurities, a realistic description of the disorder in BSCCO has to take into account the in-plane native defects with concentration estimated as 0.2% from STM. These defects are usually modeled as pointlike unitary impurities located within the CuO_2-planes. The 6th column of Fig. 2 displays the power spectrum resulting from the combined effect of the extended τ_1- and τ_3-scatterers, as displayed in the 5th column of Fig. 2, plus 0.2% pointlike unitary impurities (here V=3.9eV). The existence of native defects within the CuO_2-planes of BSCCO is only of minor importance for the high-frequency power spectrum, because their concentration is much smaller than that of the out-of-plane defects. At smaller frequencies, however, the strong pointlike impurities produce additional large-momentum features, especially close to (π,π). This is precisely what is observed in experiment: large-momentum octet vectors are only observed at low frequencies. The reason why the large-momentum features appear only at low energies can be understood from Fig. 3, where the power spectrum along the Brillouin zone diagonal is compared for a single unitary pointlike scatterer with the power spectrum resulting from a single weak extended scatterer. Note, that the intensity of the large-momentum peak, which results from the pointlike unitary scatterers, is almost frequency independent (see Fig. 3). However, its weight relative to the small-momentum features of FTSTS signal decreases for large bias values. This occurs mainly because the intensity of the low momentum features, contributed by the weak scatterers, grows rapidly with frequency.

Overall, the power spectrum calculated within our realistic disorder model (6th column in Fig. 2) reproduces the experimental one (7th column in Fig. 2) very well. This allows us to interpret some of the key features of the experimental power spectrum in the following way: (i) the dominant $\mathbf{q}_1$-peaks arise mainly from scattering by the order parameter modulations, i.e., by τ_1-scattering, (ii) the broadness of the $\mathbf{q}_7$-peaks, which are quite pronounced at small energies, is caused by poorly screened out-of-plane potential impurities, which act as extended τ_3-scatterers, (iii) the large momentum features at small frequencies originate from the in-plane native defects, which are modeled as pointlike unitary scatterers.

IV. CONCLUSIONS

We have suggested that a realistic model for the out-of-plane disorder in BSCCO-2212 should include: (i) order parameter inhomogeneities, which we have previously attributed to the fact that the oxygen dopant atoms modulate the pair interaction locally [31] and which result in enhanced Andreev or τ_1-scattering, (ii) extended weak potential or τ_3-scatterers, which could originate e.g. from the random substitution of Sr by Bi and which are spatially extended due to poor screening within the CuO_2-planes. In combination with the 0.2% in-plane native defects observed by STM, which we model as pointlike unitary potential scatterers, our model for the out-of-plane disorder is able to reproduce the essential characteristics of the experimental Fourier transform patterns in BSCCO. The fact that the out-of-plane scatterers are spatially extended explains the absence of large-momentum octet peaks and the suppression of "background" features at higher energies. The large-momentum features at small energies are caused by the 0.2% pointlike strong in-plane scatterers. The $\mathbf{q}_7$-peaks are broadened considerably due to enhanced forward scattering caused by the spatially extended potential impurities. The τ_1-scattering, which arises from the order parameter inhomogeneities observed in BSCCO, strongly enhances the dispersive $\mathbf{q}_1$-peaks especially at higher energies. The reason why τ_1-scattering mostly contributes to $\mathbf{q}_1$-peaks is a simple consequence of the d-wave symmetry of the corresponding scattering matrix elements.

The agreement of the qualitative features of the power spectrum predicted by the model introduced in Ref. [31] for the out-of-plane O dopants with experiment is further evidence in support of the contention put forward there that the O defects in the BSCCO-2212 system are actually modulating the pair interaction g locally. Of course comparisons of this type cannot directly determine the microscopic origin of the modulation of g, but since the experimental data with which we compare are from slightly overdoped samples, it seems unlikely that significant inhomogeneity is being driven by competition with a second order parameter. This therefore suggests that an atomic-scale modulation of electronic hopping parameters or electron-phonon coupling constants is indeed taking place in these materials near the dopant atoms.[31].

Acknowledgements. The authors acknowledge valuable conversations with W.A. Atkinson, A.V. Balatsky, J.C. Davis, J. Lee and K. McElroy. We would especially like to thank J.C. Davis, J. Lee and K. McElroy for sharing with us their data. Partial support for this research (BMA, TSN and PJH) was provided by ONR N00014-04-0060. TSN was supported by a Feodor-Lynen Fellowship from the A. v. Humboldt Foundation, and AM by the Institute for Fundamental Theory of the University of Florida.

[1] A. Yazdani, C. M. Howald, C. P. Lutz, A. Kapitulnik, and D. M. Eigler, Phys. Rev. Lett. **83**, 176 (1999).
[2] E. W. Hudson, S. H. Pan, A. K. Gupta, K.-W. Ng, and J. C. Davis, Science **285**, 88 (1999).
[3] S. H. Pan, E. W. Hudson, K. M. Lang, H. Eisaki, S. Uchida, and J. C. Davis, Nature **403** 746 (2000).
[4] T. Cren, D. Roditchev, W. Sacks, J. Klein, J.-B. Moussy, C. Deville-Cavellin, and M. Laguës, Phys. Rev. Lett. **84**, 147 (2000).
[5] S.-H. Pan, J. P. O'Neal, R. L. Badzey, C. Chamon, H. Ding, J. R. Engelbrecht, Z. Wang, H. Eisaki, S. Uchida, A. K. Gupta, K.-W. Ng, E. W. Hudson, K. M. Lang, and J. C. Davis, Nature **413**, 282 (2001).
[6] K. M. Lang, V. Madhavan, J. E. Hoffman, E. W. Hudson, H. Eisaki, S. Uchida, and J. C. Davis, Nature **415**, 412 (2002).
[7] C. Howald, P. Fournier, and A. Kapitulnik, Phys. Rev. B **64**, 100504(R) (2001).
[8] J. E. Hoffman, E. W. Hudson, K. M. Lang, V. Madhavan, H. Eisaki, S. Uchida, and J. C. Davis, Science **295**, 466 (2002).
[9] C. Howald, H. Eisaki, N. Kaneko, and A. Kapitulnik, cond-mat/0201546 (unpublished).
[10] C. Howald, H. Eisaki, N. Kaneko, M. Greven, and A. Kapitulnik, cond-mat/0208442 (unpublished).
[11] E. W. Hudson, V. Madhavan, K. McElroy, J. E. Hoffman, K. M. Lang, H. Eisaki, S. Uchida, and J. C. Davis, Physica B **329**, 1365 (2003).
[12] K. McElroy, R. W. Simmonds, J. E. Hoffman, D.-H. Lee, J. Orenstein, H. Eisaki, S. Uchida, and J. C. Davis, Nature **422**, 592 (2003).
[13] K. McElroy, D.-H. Lee, J. E. Hoffman, K. M. Lang, E. W. Hudson, H. Eisaki, S. Uchida, J. Lee, and J.C. Davis, cond-mat/0404005 (unpublished).
[14] N. Momono, A. Hashimoto, Y. Kobatake, M. Oda, and M. Ido, cond-mat/0505254 (unpublished).
[15] P. Sprunger, L. Petersen, E. W. Plummer, E. Lægsgaard, and F. Besenbacher, Science **275**, 1764 (1997).
[16] J. Friedel, Phil. Mag. **43**, 153 (1952).
[17] D. Zhang and C. S. Ting, Phys. Rev. B **67**, 100506(R)

(2003).
[18] Q.-H. Wang and D.-H. Lee, Phys. Rev. B **67**, 020511(R) (2003).
[19] B. M. Andersen and P. Hedegård, Phys. Rev. B **67**, 172505 (2003).
[20] D. Zhang and C. S. Ting, Phys. Rev. B. **69**, 012501 (2004).
[21] T. Pereg-Barnea and M. Franz, Phys. Rev. B **68**, 180506(R) (2003).
[22] R. S. Markiewicz, Phys. Rev. B **69**, 214517 (2004).
[23] U. Chatterjee, M. Shi, A. Kaminski, A. Kanigel, H. M. Fretwell, K. Terashima, T. Takahashi, S. Rosenkranz, Z. Z. Li, H. Raffy, A. Santander-Syro, K. Kadowaki, M. R. Norman, M. Randeria, and J. C. Campuzano, cond-mat/0505296 (unpublished).
[24] K. McElroy, G.-H. Gweon, J. Graf, S. Y. Zhou, T. Sasagawa, H. Eisaki, H. Takagi, S. Uchida, D.-H. Lee, and A. Lanzara, cond-mat/0505333 (unpublished).
[25] L. Capriotti, D. J. Scalapino, and R. D. Sedgewick, Phys. Rev. B **68**, 014508 (2003).
[26] L.-Y. Zhu, W. A. Atkinson, and P. J. Hirschfeld, Phys. Rev. B **69**, 060503(R) (2004).
[27] L. Dell'Anna, J. Lorenzana, M. Capone, C. Castellani, and M. Grilli, Phys. Rev. B **71**, 064518 (2005).
[28] H. Eisaki, N. Kaneko, D. L. Feng, A. Damascelli, P. K. Mang, K. M. Shen, Z.-X. Shen, and M. Greven, Phys. Rev. B **69**, 064512 (2004).
[29] G. Kinoda, H. Mashima, K. Shimizu, J. Shimoyama, K. Kishio, and T. Hasegawa, Phys. Rev. B **71**, 020502(R) (2005).
[30] K. McElroy, H. Eisaki, S. Uchida, and S. C. Davis, Science **309**, 1048 (2005).
[31] T. S. Nunner, B. M. Andersen, A. Melikyan, and P. J. Hirschfeld, cond-mat/0504693 (unpublished).
[32] A. Ghosal, A. Kopp, and S. Chakravarty, cond-mat/0412241 (unpublished).
[33] J.-X. Zhu, K. McElroy, J. Lee, T. P. Deveraux, Q. Si, J. C. Davis, and A.V. Balatsky, cond-mat/0507621 (unpublished).
[34] A. C. Fang, L. Capriotti, D. J. Scalapino, S. A. Kivelson, N. Kaneko, M. Greven, and A. Kapitulnik, cond-mat/0508253 (unpublished).
[35] J.-X. Zhu, cond-mat/0508646 (unpublished).
[36] B .M. Andersen, A. Melikyan, T. S. Nunner, and P. J. Hirschfeld, cond-mat/0507661 (unpublished).
[37] T. S. Nunner and P. J. Hirschfeld, Phys. Rev. B **72**, 014514 (2005).
[38] M. R. Norman, M. Randeria, H. Ding and J. C. Campuzano, Phys. Rev. B **52**, 615 (1994).
[39] Note we use the term "power spectrum" for the square root of the conventional definition.